AGU PUBLICATIONS

JGR

Journal of Geophysical Research: Oceans

RESEARCH ARTICLE

10.1002/2013JC009762

Key Points:
- Significantly higher NCP in the polynyas than sea ice zones
- Strong temporal variation in NCP between January and February
- The variation is due to the combined effect of SST, light, and Fe availabilities

Correspondence to:
D. Hahm,
hahm@kopri.re.kr

Citation:
Hahm, D., T. S. Rhee, H.-C. Kim, J. Park, Y.-N. Kim, H. C. Shin, and S. H. Lee (2014), Spatial and temporal variation of net community production and its regulating factors in the Amundsen Sea, Antarctica, *J. Geophys. Res. Oceans*, *119*, 2815–2826, doi:10.1002/2013JC009762.

Received 20 DEC 2013
Accepted 10 APR 2014
Accepted article online 20 APR 2014
Published online 13 MAY 2014

Spatial and temporal variation of net community production and its regulating factors in the Amundsen Sea, Antarctica

Doshik Hahm[1], Tae Siek Rhee[1], Hae-Cheol Kim[2], Jisoo Park[1], Young-Nam Kim[1,3], Hyoung Chul Shin[1], and SangHoon Lee[1]

[1]Korea Polar Research Institute, Incheon, Korea, [2]I.M.Systems Group at Environmental Modeling Center, NCEP/NOAA, College Park, Maryland, USA, [3]Now at Korea Marine Environment Management Corp., Seoul, Korea

Abstract We observed $\Delta O_2/Ar$ in the surface waters of the Amundsen Sea, Antarctica, during the austral summers in 2011 and 2012 to investigate the variability of net community production (NCP). Corresponding to the typical peak phytoplankton bloom period, the $\Delta O_2/Ar$ of the Amundsen Sea Polynya (ASP) reached 30% in early January 2011 and had a strong positive correlation with the sea surface temperature (SST) and chlorophyll-a (Chl-*a*). In contrast, $\Delta O_2/Ar$ decreased to −10% in the sea ice zone (SIZ), which was likely associated with either net O_2 consumption in the unlit area or the entrainment of deep water containing low dissolved oxygen. Near the terminal stage of the phytoplankton bloom in late February 2012, we observed the same contrasting $\Delta O_2/Ar$ features between the ASP and SIZ. However, the $\Delta O_2/Ar$ in the ASP was not >10%, which corresponded with the overall reduction in Chl-*a*, solar radiation, and SST compared with the corresponding values in 2011. The average net community production in the ASP was 119 ± 79 mmol O_2 m^{-2} d^{-1} in January 2011, and 23 ± 14 mmol O_2 m^{-2} d^{-1} in February 2012. The strong correlations of NCP with SST and mixed layer depth (MLD) indicate that the ASP phytoplankton bloom is likely initiated by a combination of increased light availability and SST in early summer. Low SST and variable fluorescence to maximum florescence ratio (Fv/Fm) in February indicate that decreased solar radiation and Fe availability are likely responsible for the phytoplankton bloom demise.

1. Introduction

Primary production in the Southern Ocean, which is characterized by high nutrient and low chlorophyll (HNLC) concentrations, is limited by low dissolved iron (Fe) concentrations [*Boyd et al*., 2000; *Cassar et al*., 2007]. However, the Antarctic continental shelf seas are provided with Fe from various sources, e.g., seafloor sediments, sea ice, and glacial melting [*Sedwick and DiTullio*, 1997; *Coale et al*., 2005; *Gerringa et al*., 2012]. On the continental shelf, ecosystems in the coastal polynyas have more favorable light conditions than those in the surrounding sea ice zones. Therefore, these regions host large phytoplankton blooms during the austral summer, responsible for 65% of the total primary production occurring in the Antarctic continental shelf [*Arrigo and van Dijken*, 2003].

The Amundsen Sea hosts two of the most productive coastal polynyas among the Antarctic polynyas: the Amundsen Sea Polynya (ASP) and Pine Island Bay Polynya (PIBP) [*Arrigo and van Dijken*, 2003]. Our understanding of phytoplankton bloom magnitude and timing and high primary production in the polynyas is largely based on satellite data analysis because there are insufficient in situ observations. *Arrigo et al*. [2012] demonstrated that primary production in the polynyas increases by late November in conjunction with the decreasing sea ice cover and peaks in early January (often >1.5 g C m^{-2} d^{-1}). Interestingly, the primary production begins to decrease in mid-January, whereas the polynyas continue to expand until late February. *Arrigo et al*. [2012] speculated that this phenomenon is a result of either nutrient limitations or higher zooplankton grazing pressure in mid-January. The situation in the PIBP appears to be consistent with nutrient limitations; *Gerringa et al*. [2012] argued that macronutrients and dissolved Fe were almost completely exhausted during the phytoplankton bloom. *Arrigo et al*. [2012] also found that primary production in the polynyas exhibited significant interannual variability and was positively correlated with the polynya sizes. They also suggested that the polynya sizes of the ASP and PIBP are controlled by the easterly and southerly wind strengths that push sea ice away from the coast. Larger areas of open water in

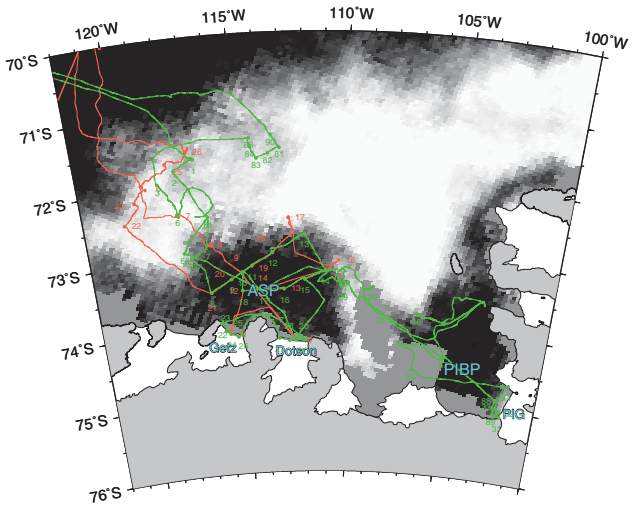

Figure 1. Cruise tracks of the IBRV Araon in the austral summers of 2011 (red line) and 2012 (green line) superimposed on a sea ice concentration map of 21 February 2012. The numbers designate the CTD stations for each cruise.

the polynyas were found in the years that exhibited larger anomalies in the easterly and southerly surface winds.

High-frequency measurements of $\Delta O_2/Ar$ using mass spectrometry [*Tortell*, 2005; *Cassar et al*., 2009] provide an opportunity to investigate net community production (NCP), which is defined as the difference between net primary production and heterotrophic respiration, with high spatial resolution. Such high-resolution NCP measurements can be considered a real-time proxy of primary production and can be compared with environmental parameters to investigate the primary production controls. *Tortell et al*. [2012] reported that Chl-*a* and $\Delta O_2/Ar$ were strongly correlated with both high SSTs and shallow mixed layer depths (MLDs) in the Amundsen Sea. They hypothesized that the strong correlation might reflect (1) time-integrated surface heat flux effects in which the higher SSTs indicate longer surface exposure, (2) effects of warm and nutrient-rich modified circumpolar deep water (MCDW) upwelling, or (3) enhanced phytoplankton metabolic rates driven by higher SSTs.

We conducted underway measurements of $\Delta O_2/Ar$ and environmental parameters on board Araon, the Korean icebreaker, during her two expeditions to the Amundsen Sea in the 2011 and 2012 austral summers (Figure 1). The goals of this study were to map the spatial and temporal NCP variations in the Amundsen Sea and to identify the NCP regulating factors to better understand the mechanisms controlling the phytoplankton bloom magnitude and timing in the polynyas of the Amundsen Sea.

2. Methods

2.1. NCP From O_2/Ar Measurements

Dissolved oxygen concentration in the mixed layer is the sum of the O_2 derived from biological (respiration and photosynthesis) and physical (dissolution of air, bubble injection, and changes in water temperature and air pressure) processes. Because Ar and O_2 have similar solubilities and diffusivities and Ar is biologically inert, the amount of biologically derived O_2 can be isolated by measuring the O_2/Ar ratio [*Craig and Hayward*, 1987; *Cassar et al*., 2009]. For the temperature (-1.9 to 0.5°C) and salinity (33–33.8) ranges that are typically observed in the Amundsen Sea surface waters, the ratios of solubility and diffusivity for O_2 and Ar vary by $<0.1\%$ and 0.01%, respectively. The biological oxygen supersaturation is defined as follows

$$\Delta O_2/Ar \equiv \frac{(O_2/Ar)_{sample}}{(O_2/Ar)_{sat}} - 1, \quad (1)$$

where $(O_2/Ar)_{sample}$ and $(O_2/Ar)_{sat}$ are the ratios of O_2/Ar in the sampled and air-saturated water, respectively. Gas exchange across the surface water-air interface that results from O_2 supersaturation becomes equivalent to NCP (in units of mmol O_2 m^{-2} d^{-1}) under the steady state condition

$$NCP = k_{O2} \cdot \rho \cdot [O_2]_{sat} \cdot \Delta(O_2/Ar), \quad (2)$$

where k_{O2} and $[O_2]_{sat}$ are the O_2 gas transfer velocity and saturated concentration, respectively, and ρ is surface water density. The calculated NCP values represent the rates integrated over the characteristic mixed layer gas

Table 1. NCP Estimates Based on $\Delta O_2/Ar$ Measurements[a]

Region	Month	NCP[b]	Source
ASP	January	119 ± 79	This study
ASP	February	23 ± 14	This study
PIBP	February	7 ± 4	This study
Ross Sea	November	-139 ± 215[c]	*Tortell et al.* [2011]
Ross Sea	December–January	52 ± 58[c]	*Tortell et al.* [2011]
Subantarctic zone	February	43 (0–180)	*Cassar et al.* [2011]
West Antarctica Peninsula	January	3–76	*Huang et al.* [2012]

[a]ASP: Amundsen Sea Polynya; PIBP: Pine Island Bay Polynya.
[b]In units of mmol O_2 m^{-2} d^{-1}, equivalent to 0.00857 g C m^{-2} d^{-1} (section 2.1).
[c]O_2 flux including negative values. The values could be negatively biased as a result of vertical mixing.

exchange time, the ratio of MLD and gas transfer velocity [*Kaiser et al.*, 2005]. The gas exchange time in the ASP was typically around 20 days. Whenever necessary, we adopted a factor of 0.00857 g C m^{-2} d^{-1}/mmol O_2 m^{-2} d^{-1} to convert NCP units, assuming a photosynthetic quotient of 1.4 for new production [*Laws*, 1991].

The O_2/Ar measurements were performed on board using an equilibrator inlet mass spectrometry system (EIMS) [*Cassar et al.*, 2009]. Surface water at a depth of 7 m was pumped into the laboratory and equilibrated with the headspace in a Weiss-type equilibrator. The O_2/Ar of the equilibrated air was measured in a quadrupole mass spectrometer and calibrated every 3–6 h against the O_2/Ar of ambient air supplied from the foremast. The O_2/Ar ratios in the Amundsen Sea continental shelf were surveyed from 30 December 2010 to 8 January 2011 and from 9 February 2012 to 6 March 2012 (Figure 1).

Because ΔO_2/Ar depends on prior wind speeds at the observation time, we used the weighted gas transfer velocity [*Reuer et al.*, 2007, equation (6)] rather than the instantaneous gas transfer velocity. The weighted gas transfer velocity represents the average of the gas transfer velocities during the 60 days prior to the observation date, weighted heavily for several days closest to the observation date [see *Reuer et al.*, 2007 for details]. The NCEP daily wind speeds at 10 m above the sea surface, which were fed to the parameterization of *Wanninkhof* [1992], and the climatological MLDs [*Levitus and Boyer*, 1994] were used as inputs in the calculation of the weighted gas transfer velocity. In practice, the mean ASP NCPs (Table 1) that were calculated from the weighted gas transfer velocity were not significantly different from the values determined using the instantaneous gas transfer velocity (*t* test, $p < 0.002$). The O_2 and Ar solubilities were determined according to *Garcia and Gordon* [1992] and *Hamme and Emerson* [2004], respectively.

2.2. Ancillary Measurements

Sea surface temperature and salinity were measured underway using a thermosalinograph (SBE45). Fluorescence, which is a Chl-*a* indicator, was measured using a Turner Designs 10-AU equipped with a continuous flow cuvette and calibrated against Chl-*a* concentrations determined from discrete water samples by fluorometry. Sea ice concentrations along the ship track were derived from AMSR-E and SSM/I daily sea ice maps for 2011 and 2012, respectively [*Spreen et al.*, 2008]. The along-track sea ice concentrations shown in Figures 2a and 2e are averages of the data points (typically 8–9 points) within 10 km of the ship position on a daily sea ice map (e.g., gray background maps in Figure 1). MLDs ($\Delta\sigma_t = 0.05$ kg m^{-3} criterion) [*Rintoul and Trull*, 2001] and euphotic depths (1% of the surface irradiance) were also calculated at the stations where vertical CTD casts were made (Figure 1). Variable fluorescence measurements of discrete water samples were made using a fluorescence induction and relaxation (FIRe) fluorometer. The seawater samples were dark-light or low-light adapted for 30 min before measuring the quantum efficiencies of the PSII (Fv/Fm) [*Kolber and Falkowski*, 1993]. The measured fluorescence was corrected for the blank signal recorded from filtered seawater. Here the mean value in the mixed layer was used as a proxy for Fe availability [*Hopkinson et al.*, 2007; *Cassar et al.*, 2011].

3. Results

3.1. Peak Bloom Observations in 2011

3.1.1. Amundsen Sea Polynya (ASP)

Early January corresponds to the typical peak phytoplankton bloom in the ASP [*Arrigo et al.*, 2012]. At this time, the sea surface temperature in the ASP was considerably higher than the surrounding sea ice zone

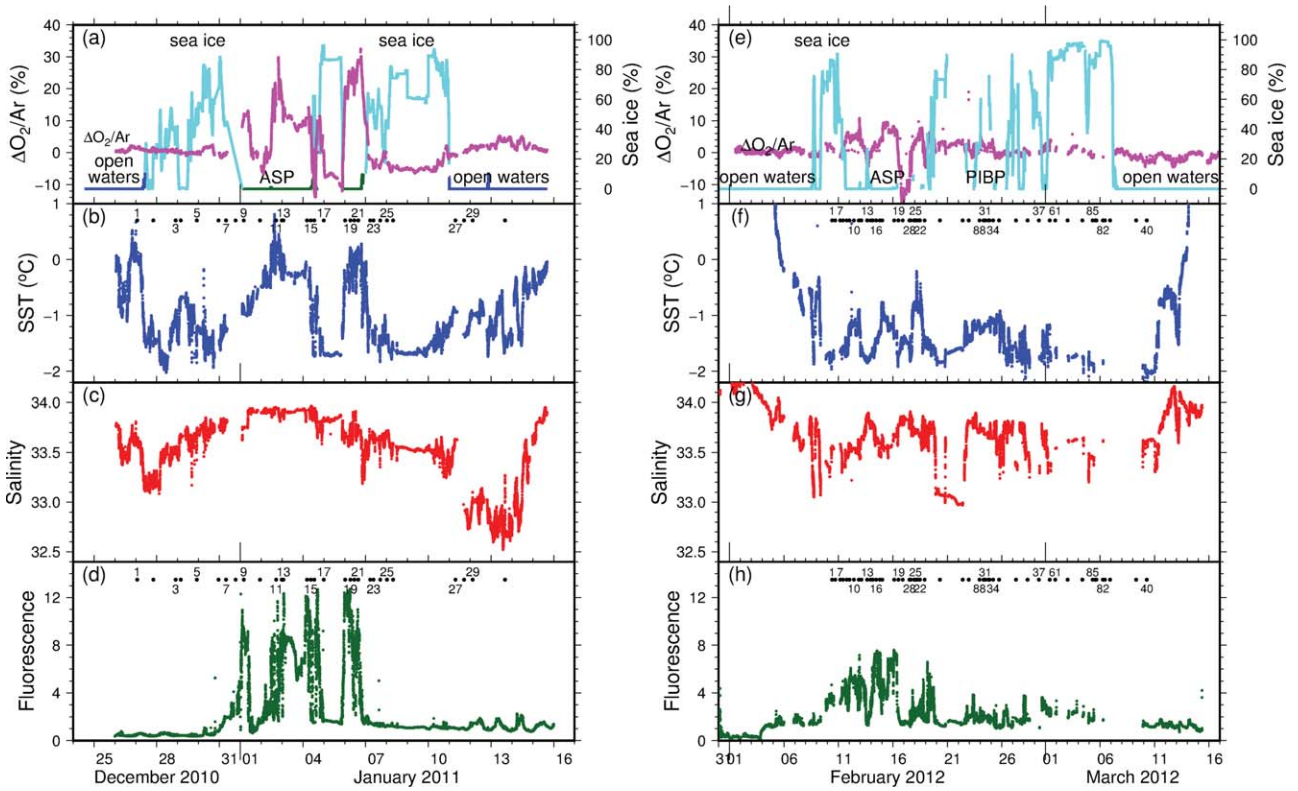

Figure 2. Time series of (a) the $\Delta O_2/Ar$ and sea ice concentration, (b) sea surface temperature, (c) salinity, and (d) fluorescence in 2011. The same parameters in 2012 are shown in the right column. Numbers and dots in the SST and fluorescence plots indicate the CTD stations on the corresponding dates.

(SIZ), ranging from −1.4 to 1.0°C and averaging 0.4 ± 0.4°C (Figure 2b), because the polynya is exposed to enhanced radiant flux from prolonged daylight in midsummer. Salinity in the ASP was slightly higher than in the SIZ, ranging from 33.2 to 34.0 and averaging 33.8 ± 0.1.

Underway fluorescence in the ASP exhibited a relatively large variation, i.e., 1–14 μg/L (5.7 ± 3.2 μg/L; Figure 2d). The high fluorescence region corresponded spatially with the high-temperature region. Similarly, $\Delta O_2/Ar$ in the ASP exhibited a broad range of −7 to 30% (11.7 ± 9.9%; Figure 2a). High $\Delta O_2/Ar$ values were found in regions with high temperature and fluorescence. Moreover, negative $\Delta O_2/Ar$ ratios often coincided with low temperature and fluorescence. Specifically, the lowest $\Delta O_2/Ar$ in the waters ahead of the Dotson Ice Shelf was −7% (Figures 2a and 3d).

3.1.2. Sea Ice Zone (SIZ)

The SIZ was considerably cooler than the ASP, ranging between −1.8 and 0°C (average of −1.0 ± 0.5°C), likely due to limited solar radiation. Salinity in the SIZ exhibited a broader range compared with the ASP; the lowest salinity was 33.3. The lower salinity in the SIZ compared with that of the polynya was likely a result of the thawing sea ice in the SIZ.

Fluorescence and $\Delta O_2/Ar$ in the SIZ were both lower than in the ASP. The fluorescence values typically did not exceed 4 μg/L, and many $\Delta O_2/Ar$ values were less than zero (4.8 ± 8.1%). This finding indicates that primary production in the SIZ is considerably weaker than in the ASP. Moreover, the small biological O_2 supersaturation is often overwhelmed by persistent influence of the waters near the SIZ, which accumulated a high respiratory signal during the winter due to restricted air-sea gas exchange under the sea ice.

3.2. Declining Bloom Observations in 2012

3.2.1. Amundsen Sea Polynya (ASP)

In February 2012, the overall sea surface waters were considerably colder than in 2011 (Figures 2b and 3e). The average SST observed in late February (−1.4 ± 0.3°C) was substantially colder than that observed in

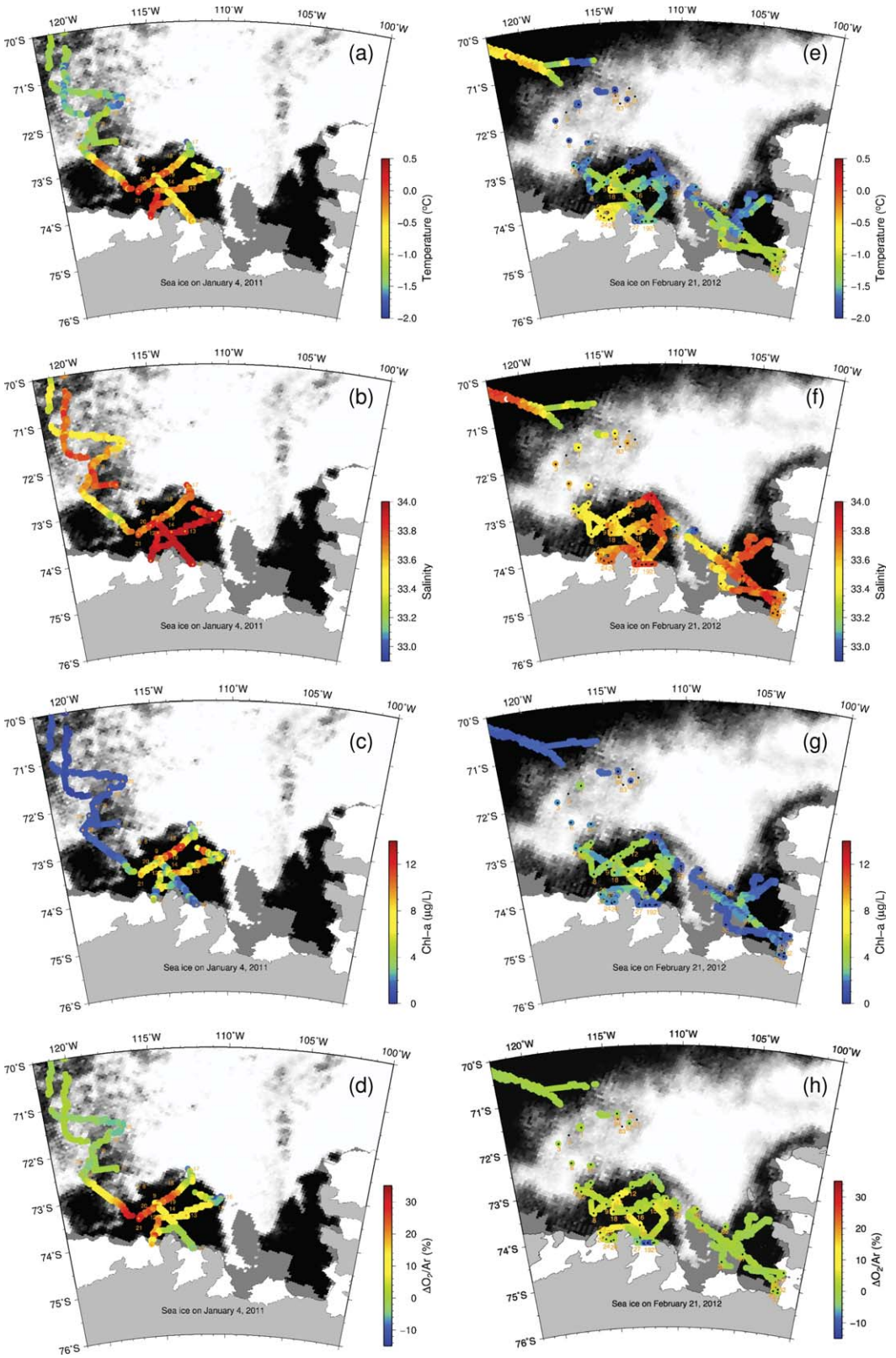

Figure 3. Spatial distributions of (a) temperature, (b) salinity, (c) fluorescence, and (d) $\Delta O_2/Ar$ in the Amundsen Sea in 2011. The same parameters are shown in the right column for 2012. The ASP exhibited higher temperature, fluorescence, and $\Delta O_2/Ar$ compared with the surrounding SIZs.

early January 2011 (0.4 ± 0.4°C). This difference is likely related to the reduction in solar radiation and shortened daylight periods.

The higher SST ahead of the Getz Ice Shelf compared with the Dotson Ice Shelf was consistent throughout both early January and mid-February in the ASP. This finding might be attributed to the warm and saline MCDW entrainment into the surface waters. However, this phenomenon did not occur in our observation periods. Instead, the CTD casts along the shelves in 2012 (not shown) revealed increased MCDW entrainment ahead of the Dotson Ice Shelf, which was more prominent along the western side of the shelf. This feature cannot be attributed to solar radiation either. Satellite sea ice concentration images (AMSR-E and SSM/I for 2011 and 2012, respectively) indicated that the sea ice ahead of the Dotson Ice Shelf melted earlier than the sea ice ahead of the Getz Ice Shelf. Determining a direct cause for the different SSTs and $\Delta O_2/Ar$ values of the two ice shelves was challenging based on the current data set. The average salinity in 2012 (33.6 ± 0.1) was slightly lower than that in 2011 (33.8 ± 0.1; Figure 3f).

Higher underway fluorescence values in the ASP compared with the SIZ were persistent in 2012. However, the magnitude was smaller, decreasing from 5.7 ± 3.2 μg/L in 2011 to 3.7 ± 1.4 μg/L in 2012 (Figure 3g). Similarly, the average $\Delta O_2/Ar$ value decreased from 11.7 ± 9.9% in 2011 to 3.8 ± 3.1% in 2012.

3.2.2. Sea Ice Zone (SIZ)

Similar to the ASP, the average temperature in the SIZ decreased significantly from −1.0°C in 2011 to −1.6°C in 2012. By contrast, the average salinity (33.6) was the same in both 2011 and 2012. The average fluorescence was 2.8 ± 1.1 μg/L in 2012, which was similar to the fluorescence observed in 2011 (2.3 ± 1.4 μg/L). The average $\Delta O_2/Ar$ decreased slightly from 4.8% in 2011 to 2.2% in 2012. Additionally, unlike 2011, which exhibited a wide range from −10 to 20%, most $\Delta O_2/Ar$ values fell between 0 and 8% in 2012.

3.2.3. Pine Island Bay Area (PIBP and SIZ-E)

In 2012, the Pine Island Bay area east of 110°W was also surveyed. The average SSTs in the polynya (PIBP) and adjacent SIZ (SIZ-E) were −1.4 ± 0.2 and −1.5 ± 0.2°C, respectively, which were not significantly different from those in the ASP and SIZ. The average salinities in the PIBP and SIZ-E were both 33.7, which was slightly higher than the average of 33.6 in the ASP and SIZ. Interestingly, the average fluorescence in Pine Island Bay (both PIBP and SIZ-E were <2 μg/L) was significantly lower than that observed in the ASP and SIZ regions. Moreover, the $\Delta O_2/Ar$ in the PIB area rarely exceeded 5%, and the average was nearly zero. This near-equilibrium state (i.e., insignificant net biological O_2 production) is not surprising given that the observation period (24–27 February 2012) occurred after the typical phytoplankton bloom termination around 20 February in the PIBP, and the PIBP has a shorter phytoplankton bloom duration and less net primary production than the ASP [*Arrigo et al*., 2012].

4. Discussion

4.1. NCPs in the Polynyas

The calculated NCPs were spatially averaged with a 5 km by 5 km resolution to reduce potential bias from highly sampled regions due to variable ship speeds. In practice, this bias was relatively small in our observations. For example, the NCP "raw" mean (i.e., before spatial averaging) in the ASP in 2011 was 112 ± 68 mmol O_2 m^{-2} d^{-1} (n = 3822), which was nearly identical to the spatially averaged value of 119 ± 68 mmol O_2 m^{-2} d^{-1} (n = 148). To deduce the regionally averaged NCPs (Table 1), only the positive values were selected because the negative values, which are largely found in sea ice zones, may not represent the heterotrophic conditions in the studied areas. Instead, these values may represent footprints of wintertime-accumulated respiration that have not yet been completely compensated by the summertime net O_2 production [*Cassar et al*., 2011]. A similar explanation is likely applicable to the extremely low O_2 fluxes observed in the Ross Sea in November (−139 ± 215 mmol O_2 m^{-2} d^{-1}) [*Tortell et al*., 2011]. NCPs in sea ice zones were not reported in Table 1 because these values might be influenced by O_2 deficit caused by remineralization during winter and gas exchange through sea ice is not well constrained. *Loose et al*. [2009], for instance, reported that the gas flux through sea ice pack might not scale linearly with open water area. However, the influences of O_2 deficit and limited gas exchange should be minimal on the NCP values in the polynya. Because the ASP typically opens on 11 November and the characteristic mixed layer gas exchange time is approximately 20 days, the ASP should be free of O_2 deficit caused by the winter remineralization and reveal O_2 supersaturation produced by biological activity at the time of our observations in January

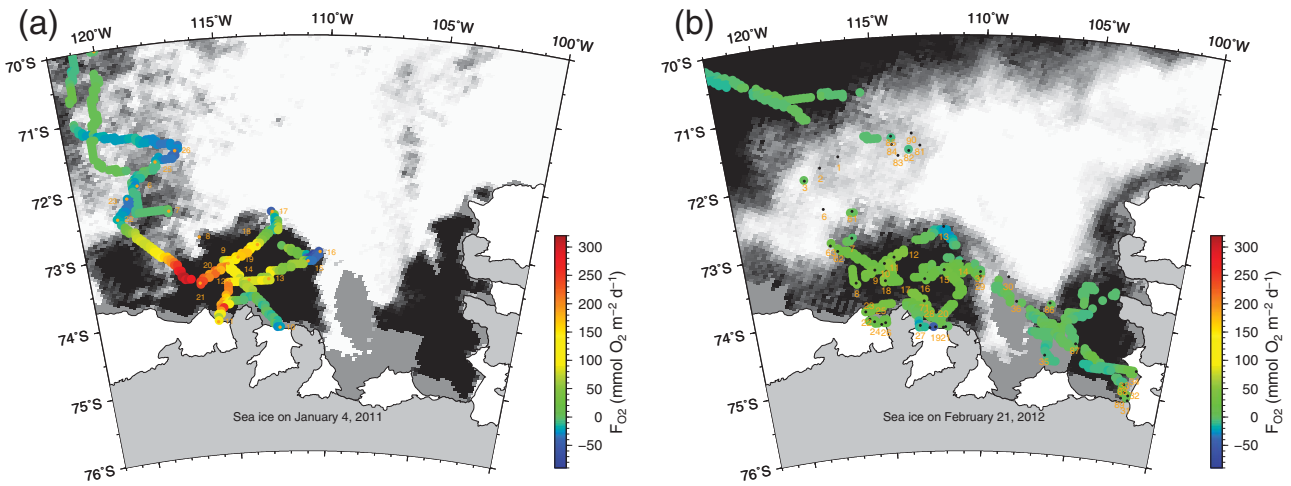

Figure 4. NCPs in (a) 2011 and (b) 2012. NCPs in the ASP were much higher than in the surrounding SIZs in 2011. However, the spatial contrast between the ASP and SIZ was considerably smaller in 2012 than in 2011 (see the text).

and February. Generally, the reduced confidence in the NCPs in the SIZs leads us to focus on NCPs in the polynyas in the following discussion.

Tortell et al. [2012] observed $\Delta O_2/Ar$ values in the Amundsen Sea from 11 January 2009 to 16 February 2009 were largely focused on the Pine Island Bay and adjacent areas. The observed $\Delta O_2/Ar$ values were between −40% and 40% (mean of 8.6%). During our on-shelf observation period from 30 December 2010 to 8 January 2011, $\Delta O_2/Ar$ values ranged from −12% to 32% (mean of 10.4%). Both *Tortell et al.* [2012] and our observations covered typical high-bloom periods in early January and suggested similar $\Delta O_2/Ar$ values, indicating that the NCPs in the ASP and PIBP areas are comparable. The similarity is not surprising given that *Arrigo and van Dijken* [2003] observed through satellite data that primary production was similar in the ASP and PIBP (2.11 and 2.08 g C m^{-2} d^{-1}, respectively). *Lee et al.* [2012] also reported a similar value (2.2 ± 1.4 g C m^{-2} d^{-1}) in the ASP in January 2011.

The Ross Sea and Amundsen Sea appear to have similar NCPs. *Tortell et al.* [2011] measured $\Delta O_2/Ar$ in the Ross Sea from December 2005 to January 2006 and reported a mean flux of 52.2 ± 58.3 mmol O_2 m^{-2} d^{-1}, including both positive and negative fluxes. The mean flux (63 ± 87 mmol O_2 m^{-2} d^{-1}) for both ASP and SIZ in the Amundsen Sea in January 2011 was similar to observations from the Ross Sea. Furthermore, the West Antarctica Peninsula (WAP) and Australian Subantarctic Zone (ASAZ) have significantly lower NCPs than the ASP in January. *Huang et al.* [2012] observed NCPs between 3 and 76 mmol O_2 m^{-2} d^{-1} on the WAP in January 2008. Moreover, *Cassar et al.* [2011] observed an average NCP of 43 mmol O_2 m^{-2} d^{-1} (0–180 mmol O_2 m^{-2} d^{-1}) in the ASAZ from January to February in 2007. Although the regional comparison indicates that the Antarctic continental polynyas provide a hot spot for NCP, it is noted that NCP values are highly dependent on the observation periods and that comparison should be made with caution (see below).

Both the WAP and ASAZ exhibited a positive correlation between NCP and Fv/Fm, which is a proxy for Fe availability [*Cassar et al.*, 2011; *Huang et al.*, 2012], suggesting that these regions were generally depleted in Fe; a modest increase in chlorophyll and NCP were observed in localities with relatively high Fe availability. This positive correlation is different from the negative correlation found in our ASP observations. This discrepancy is discussed in section 4.2.2.

A strong temporal variation is another remarkable feature found in the Amundsen Sea NCPs (Figure 4). In February 2012, the mean NCP in the ASP was 19% of the NCP from January 2011 (Table 1). This was consistent with in situ primary production measurements [*Lee et al.*, 2012, and their unpublished data], suggesting an approximate sevenfold decrease from 2.2 to 0.31 g C m^{-2} d^{-1}. *Arrigo and van Dijken* [2003] reported a rather modest nearly threefold decrease (2.7 to 1 g C m^{-2} d^{-1}) in PP between the peak phytoplankton bloom and late February.

Furthermore, the mean NCP in the PIBP was significantly lower than in the ASP, likely due to different observational periods. The observations in the ASP were made between 11 and 22 February 2012, i.e., within a

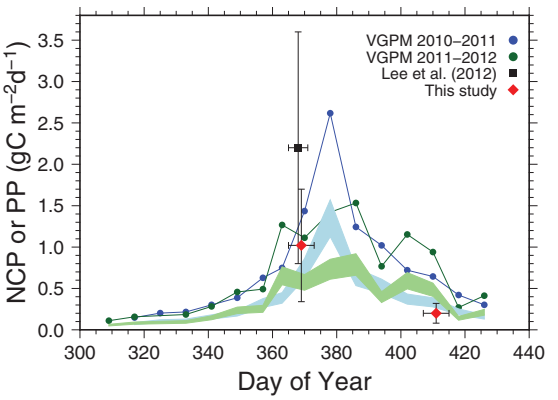

Figure 5. Comparison of satellite-based (VGPM) [*Behrenfeld and Falkowski*, 1997] and measured primary production [*Lee et al*., 2012 and this study]. Shaded blue and green areas indicate the NCP extent for 2010–2011 and 2011–2012, respectively. The lower and upper bound of the shaded areas were determined using constant *f-ratios* of 0.43 and 0.60, respectively. Vertical bars represent one standard deviation of the production measurement. Horizontal bars indicate the beginning and end of the production measurements used to produce the corresponding average.

typical bloom period in the ASP (12 December to 23 February). However, the observations in the PIBP were made between 22 and 28 February 2012, i.e., after the typical bloom period termination in the PIBP (23 December to 19 February) [*Arrigo et al*., 2012].

An attempt was made to estimate a cumulative NCP range during the bloom period in the ASP based on satellite-derived primary production (PP) time series (VGPM) [*Behrenfeld and Falkowski*, 1997] and a constant *f-ratio* during the studied period. Indeed, if we adopt the empirical equation of *Dunne et al*. [2005], which uses SST and chlorophyll as predictor variables, the *f-ratios* in January 2011 and February 2012 are 0.43 $\pm$ 0.07 (n = 8) and 0.34 $\pm$ 0.06 (n = 21), respectively, which are not statistically different from each other (*t* test, $p < 0.005$). It was also assumed that the NCP provided a good approximation of new production (NP) in steady state systems [*Falkowski et al*., 2003]. Figure 5 presents the PP in the ASP for the 2010–2011 and 2011–2012 periods. The VGPM PP was calculated by the Moderate-Resolution Imaging Spectroradiometer (MODIS) Aqua (version R2012.0)-derived Chl-*a*, SST, and PAR obtained from the Goddard Space Flight Center. Although there were some discrepancies in the magnitude and timing of the maximum PP, the cumulative PPs during the two periods ($\sim$120 days) were similar, averaging 84 and 81 g C m^{-2} for 2011 and 2012, respectively. These values are also comparable to the cumulative PP (91 $\pm$ 100 g C m^{-2}) based on both the mean PP (0.76 $\pm$ 0.86 g C m^{-2} d^{-1}) in the bloom period reported by *Arrigo and van Dijken* [2003] and the in situ production measurement of *Lee et al*. [2012] (Figure 5). *Lee et al*. [2012] reported an *f-ratio* of 0.60 $\pm$ 0.09 ($n = 5$) for the ASP based on ^{15}N uptake experiments. Alternatively, if our NCP of 119 mmol O_2 m^{-2} d^{-1} (1.02 g C m^{-2} d^{-1}) was combined with the 2.2 g C m^{-2} d^{-1} of PP suggested by *Lee et al*. [2012], the *f-ratio* would be 0.46, assuming that the O_2:C ratio is 1.4 [*Laws*, 1991] and that NCP approximates NP. Thus, the *f-ratio* in peak bloom of ASP was likely between 0.43 and 0.60, based on the empirical equation of *Dunne et al*. [2005] and the in situ measurement of *Lee et al*. [2012], respectively. If a constant *f-ratio* is assumed, NCP during the period becomes 35 and 50 g C m^{-2} with ratios of 0.43 and 0.60, respectively. Because no significant PP likely occurred other than during the bloom period in the ASP, these NCPs should approximate the annual NCPs. The annual NCPs in the ASP appear to be higher than the global average of approximately 28 g C m^{-2} yr^{-1} [*Lee*, 2001], regardless of the *f-ratio* chosen. However, we note that our estimate of cumulative NCP is highly dependent on the choice of satellite-based PP and *f-ratio*.

4.2. Correlation With Other Environmental Parameters

Correlations between the NCP and environmental parameters were investigated to identify important drivers that initiate and terminate blooms in the ASP. Ten minute averaged values of underway measurements that correspond to the CTD observation periods were calculated to facilitate the comparison with parameters that were only available via CTD observations (e.g., MLD, euphotic depth, nutrients, and Fv/Fm). We used a volumetric NCP (NCP_{vol}; mmol O_2 m^{-3} d^{-1}) [*Cassar et al*., 2011], which is defined as the ratio of NCP to MLD, rather than a depth-integrated NCP (mmol O_2 m^{-2} d^{-1}) to normalize the NCP variation caused by the variable MLD. In fact, because the MLD changed within a modest range of 20–60 m at the high NCP stations, the conversion between the depth-integrated NCP and volumetric NCP did not change the overall correlations between the NCP and other environmental parameters.

4.2.1. Light Availability and/or SST

A strong positive correlation between NCP_{vol} and SST was observed, especially at the ASP stations in peak bloom 2011 (Figure 6a). This finding is not surprising given that $\Delta O_2/Ar$ was positively correlated with the SST and fluorescence (Figures 6b and 6c) and that NCP is proportional to $\Delta O_2/Ar$ (equation (2)). The positive

correlation between the NCP (ΔO_2/Ar) and SST was also reported by *Tortell et al*. [2012]. The higher SSTs at the ASP stations were likely a result of the time-integrated surface heat flux effects, with higher SSTs indicating longer surface exposure and higher light availability, as noted by *Tortell et al*. [2012]. However, it was not clear whether the SST caused the high NCP by enhancing the phytoplankton metabolic rate. To separate the effects of SST and light availability on NCP, an independent measurement of phytoplankton growth rate at very low temperatures (−2–1°C) must be conducted.

Laws et al. [2000] predicted higher respiration rates at higher temperatures in the range of 0–20°C, implying negative correlation between NCP and SST. Considering the positive correlation between NCP and SST in the ASP and the much smaller temperature (−1.8 to 0.5°C) and spatial (the Amundsen Sea) scale, the respiration rate did not appear to vary significantly enough to influence the correlation between NCP and SST, at least among the ASP stations in 2011.

By contrast, a negative correlation was found between the MLD and NCP at stations that had high NCPs in 2011 (Figure 6d), suggesting that light availability is an important driver for high NCPs. *Cassar et al*. [2011] and *Huang et al*. [2012] found a similar negative correlation between NCP and MLD in the subantarctic ocean south of Tasmania and the WAP, respectively. Interestingly, a shallow MLD itself does not appear sufficient for producing high NCPs. For example, stations where the sea ice only began to melt (many stations in the SIZ) exhibited relatively shallow MLDs (Figure 6d) and thus high light availability. However, these stations did not exhibit high NCPs compared to the ASP stations in 2011. This result indicates that the ambient water temperature did not reach the optimum range for their metabolic rate despite the water column being stratified at sufficiently shallow depths to retain phytoplankton at well-lit depths. Therefore, the SST is not only a proxy for light availability and thermal structure in water but also an important indicator for accumulated net biological production capacity. *Tortell et al*. [2012] reported similar results; their high-productivity region with high fluorescence and ΔO_2/Ar in the PIBP was associated with relatively high SSTs and shallower MLDs.

Yet another potential explanation introduced by *Tortell et al*. [2012] suggests that high SSTs are a consequence of upwelled MCDW near ice shelves, which also carries high macronutrients and Fe concentrations that fuel biological productivity [*Gerringa et al*., 2012]. However, our observations are not consistent with this explanation. For example, two adjacent (∼50 km apart) ice shelves in the ASP, the Getz and Dotson Ice Shelves (GIS and DIS, respectively), exhibited a stark contrast in SSTs for both expeditions; the SSTs ahead of the GIS were significantly higher than those ahead of the DIS, which resulted in higher fluorescences and NCPs near the GIS compared with the DIS (Figure 3). This finding might suggest that the MCDW upwelling to the upper layers should be more pronounced in the GIS. However, our observations along the shelves in 2012 (not shown) suggested the opposite. A higher degree of mixing between the MCDW and upper layer waters along the western side of the DIS was observed, which was absent along the GIS.

4.2.2. Iron (Fe) Limitation

The HNLC conditions in the Southern Ocean are often related to an Fe limitation [*Boyd et al*., 2000; *Cassar et al*., 2007]. However, the polynyas in the Amundsen Sea are likely supplied with dissolved Fe via glacial meltwater (∼1 nM) [*Gerringa et al*., 2012]. Because Fe was not measured in the water column to assess Fe limitation in the polynyas, the NCP was instead compared with the Fv/Fm (Figures 6e and 6f). Fv/Fm is a good indicator of overall physiological stress on phytoplankton and is often related to photo-inhibition or Fe limitation in the Southern Ocean [*Kolber and Falkowski*, 1993; *Park et al*., 2013]. As our observations suggest that solar radiation enhances the overall productivity in the polynyas by providing increased light availability for light reactions in photosynthesis and/or accelerating metabolic rates (dark reactions) of phytoplankton dependent on temperature, we regard Fv/Fm as a proxy for iron limitation instead of photo-inhibition. Additionally, we found no clear correlation between the Fv/Fm and MLD, which implied that substantial photo-inhibition did not occur in the ASP and its vicinity. *Lee et al*. [2012] also found that there was no significant photo-inhibition in the Amundsen Sea.

The Fv/Fm in the Amundsen Sea ranged from 0.26 to 0.51 (Figures 6e and 6f) when the two lowest observed values in the outer shelf stations were excluded. Most of the ASP stations generally exhibited lower Fv/Fm values, i.e., $<$0.36, which was contrary to the higher values from the PIB stations, i.e., near 0.5. Although the ASP is supplied with ample Fe from glacial meltwater [*Gerringa et al*., 2012], the ASP bloom is likely temporarily limited by Fe during its high peak and shortly thereafter. On the other hand, the PIBP and

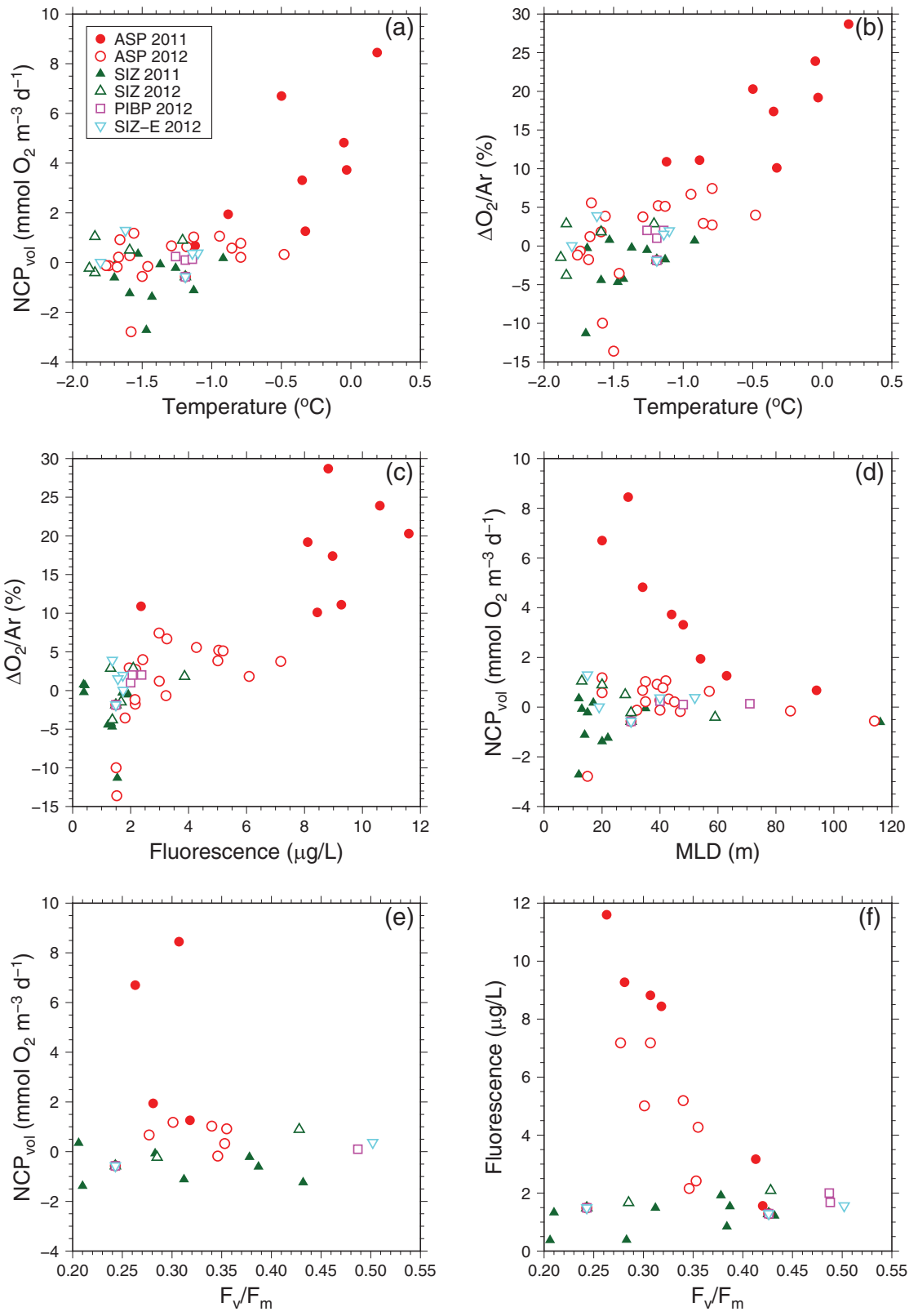

Figure 6. Relationships of volumetric NCP with environmental parameters. (a) NCP and (b) $\Delta O_2/Ar$ are positively correlated with (c) SST and fluorescence. NCP of ASP 2011 is negatively correlated with (d) MLD. (e and f) The high NCP stations at the ASP exhibited low Fv/Fm.

SIZ-E may have recovered from the Fe-limited state during the bloom period. Alternatively, the PIBP Fe supply rate may be large enough to sustain the bloom without an Fe shortage. To determine the cause of the Fv/Fm difference between the PIBP and ASP, a time series of Fv/Fm (and Fe) observations during the bloom period is required.

Our lower Fv/Fm observations for the high NCP stations differ from observations in the subantarctic zone (SAZ) and West Antarctica Peninsula (WAP). *Cassar et al*. [2011] and *Huang et al*. [2012] found that stations in their study areas with higher Fv/Fm (higher Fe availability) had higher NCP. This discrepancy may be explained by the difference in supply-consumption dynamics. In the SAZ and WAP, the Fe supply may be sufficiently large (dissolved Fe of 0.2–0.6 nM) [*Cassar et al*., 2011] to sustain the moderate biomass consumption (Chl-*a* < 1 μg/L). However, it is likely that an Fe shortage (0.04–0.1 nM) [*Gerringa et al*., 2012] occurs during the peak bloom (>10 μg/L) season, despite substantial Fe supplies from glaciers in the ASP.

In summary, the blooms in the polynyas are likely initiated by a combination of increased light availability and SSTs in the early summer, and the blooms may be fueled by Fe from glacial meltwater. In late summer, the decreased solar radiation and Fe availability are likely responsible for the bloom terminations.

5. Conclusions

To investigate NCP variability and regulating factors, $\Delta O_2/Ar$ was observed in the Amundsen Sea surface waters during the austral summers in 2011 and 2012. In early January 2011, corresponding to the typical phytoplankton bloom peak, the ASP $\Delta O_2/Ar$ ratios increased up to 30%, exhibiting strong positive correlations with SST and Chl-*a*. Strong correlations were also observed for the NCP with SST and MLD, implying that the ASP bloom was initiated by increased light availability and SST. By contrast, $\Delta O_2/Ar$ decreased to -10% in the SIZ, likely associated with either net O_2 consumption in the unlit area or entrainment of deep water with a low dissolved oxygen content. Near the terminal stage of the bloom in late February 2012, $\Delta O_2/Ar$ in the ASP was at most 10%, reflecting an overall reduction in Chl-*a*, solar radiation, and SST compared to 2011. The decreased solar radiation and Fe availability were likely responsible for the phytoplankton bloom terminations. Annual NCP in the ASP was estimated to be 35–50 g C m^{-2} based on satellite observations of the primary production temporal variation, which was nearly twice the global average.

The principal drivers of primary production may be different during each stage of the bloom cycle. Observations of $\Delta O_2/Ar$ and environmental parameters at other stages of the bloom cycle are required to better understand the NCP interannual variability and changes in the principal drivers and their ecological effects on NCP. Given that the Amundsen Sea is located in West Antarctica, where rapid ice sheet retreat occurs due to climate change, a further examination of the important parameters driving the biological bloom cycle in the polynyas should enhance our understanding of biological feedbacks to future climate change.

Acknowledgments
The authors wish to thank the captain and crew of the IBRV Araon for their assistance on board. This work was supported by grants from Korea Polar Research Institute (PE11050, PE13410, and PP13020). Comments and suggestions by two anonymous reviewers are gratefully acknowledged. The data for this paper are available at Korea Polar Data Center (http://kpdc.kopri.re.kr). Data IDs: KPDC_OSWMUEIMS_2011 and KPDC_OSWMUEIMS_2012.

References

Arrigo, K., and G. L. van Dijken (2003), Phytoplankton dynamics within 37 Antarctic coastal polynya systems, *J. Geophys. Res.*, *108*(C8), 3271, doi:10.1029/2002JC001739.

Arrigo, K. R., K. E. Lowry, and G. L. van Dijken (2012), Annual changes in sea ice and phytoplankton in polynyas of the Amundsen Sea, Antarctica, *Deep Sea Res., Part II*, *71–76*, 5–15.

Behrenfeld, M. J., and P. G. Falkowski (1997), Photosynthetic rates derived from satellite-based chlorophyll concentration, *Limnol. Oceanogr.*, *42*(1), 1–20.

Boyd, P. W., et al. (2000), A mesoscale phytoplankton bloom in the polar Southern Ocean stimulated by iron fertilization, *Nature*, *407*(6805), 695–702.

Cassar, N., M. L. Bender, B. A. Barnett, S. Fan, W. J. Moxim, H. Levy II, B. Tilbrook (2007), The Southern Ocean biological response to Aeolian iron deposition, *Science*, *317*, 1067–1070.

Cassar, N., B. A. Barnett, M. L. Bender, J. Kaiser, R. C. Hamme, and B. Tilbrook (2009), Continuous high-frequency dissolved O_2/Ar measurements by equilibrator inlet mass spectrometry, *Anal. Chem.*, *81*, 1855–1864.

Cassar, N., P. J. DiFiore, B. A. Barnett, M. L. Bender, A. R. Bowie, B. Tilbrook, K. Petrou, K. J. Westwood, S. W. Wright, and D. Lefevre (2011), The influence of iron and light on net community production in the Subantarctic and Polar Frontal Zones, *Biogeosciences*, *8*, 227–237.

Coale, K., R. Michael Gordon, and X. Wang (2005), The distribution and behavior of dissolved and particulate iron and zinc in the Ross Sea and Antarctic circumpolar current along 170 W, *Deep Sea Res., Part I*, *52*, 295–318.

Craig, H., and T. Hayward (1987), Oxygen supersaturation in the ocean: Biological versus physical contributions, *Science*, *235*(4785), 199–202.

Dunne, J. P., R. A. Armstrong, A. Gnanadesikan, and J. L. Sarmiento (2005), Empirical and mechanistic models for the particle export ratio, *Global Biogeochem. Cycles*, *19*, GB4026, doi:10.1029/2004GB002390.

Falkowski, P. G., E. A. Laws, R. T. Barber, and J. W. Murray (2003), Phytoplankton and their role in primary, new, and export production, in *Ocean Biogeochemistry, Global Change, The IGBP Ser.*, edited by M. J. R. Fasham, pp. 99–121, Springer, Berlin.

Garcia, H., and L. Gordon (1992), Oxygen solubility in seawater: Better fitting equations, *Limnol. Oceanogr.*, *37*(6), 1307–1312.
Gerringa, L. J. A., A.-C. Alderkamp, P. Laan, C.-E. Thuróczy, H. J. W. De Baar, M. M. Mills, G. L. van Dijken, H. v. Haren, and K. R. Arrigo (2012), Iron from melting glaciers fuels the phytoplankton blooms in Amundsen Sea (Southern Ocean): Iron biogeochemistry, *Deep Sea Res., Part II*, *71*, 16–31.
Hamme, R. C., and S. R. Emerson (2004), The solubility of neon, nitrogen and argon in distilled water and seawater, *Deep Sea Res., Part I*, *51*(11), 1517–1528.
Hopkinson, B. M., B. G. Mitchell, R. A. Reynolds, H. Wang, K. E. Selph, C. I. Measures, C. D. Hewes, O. Holm-Hansen, and K. A. Barbeau (2007), Iron limitation across chlorophyll gradients in the southern Drake Passage: Phytoplankton responses to iron addition and photosynthetic indicators of iron stress, *Limnol. Oceanogr.*, *52*, 2540–2554.
Huang, K., H. Ducklow, M. Vernet, N. Cassar, and M. L. Bender (2012), Export production and its regulating factors in the West Antarctica Peninsula region of the Southern Ocean, *Global Biogeochem. Cycles*, *26*, GB2005, doi:10.1029/2010GB004028.
Kaiser, J., M. K. Reuer, B. Barnett, and M. L. Bender (2005), Marine productivity estimates from continuous O_2/Ar ratio measurements by membrane inlet mass spectrometry, *Geophys. Res. Lett.*, *32*, L19605, doi:10.1029/2005GL023459.
Kolber, Z., and P. G. Falkowski (1993), Use of active fluorescence to estimate phytoplankton photosynthesis in situ, *Limnol. Oceanogr.*, *38*(8), 1646–1665.
Laws, E. A. (1991), Photosynthetic quotients, new production and net community production in the open ocean, *Deep Sea Res., Part I*, *38*(1), 143–167.
Laws, E. A., P. G. Falkowski, W. O. Smith, H. Ducklow, and J. J. McCarthy (2000), Temperature effects on export production in the open ocean, *Global Biogeochem. Cycles*, *14*, 1231–1246.
Lee, K. (2001), Global net community production estimated from the annual cycle of surface water total dissolved inorganic carbon, *Limnol. Oceanogr.*, *46*(6), 1287–1297.
Lee, S. H., B. K. Kim, M. S. Yun, H. T. Joo, E. J. Yang, Y. N. Kim, H. C. Shin, and S. H. Lee (2012), Spatial distribution of phytoplankton productivity in the Amundsen Sea, Antarctica, *Polar Biol.*, *35*, 1721–1733.
Levitus, S., and T. P. Boyer (1994), World Ocean Atlas 1994, in *NOAA Atlas NES-DIS 4, Temperature*, vol. 4, p. 117, U.S. Gov. Print. Off., Washington, D. C.
Loose, B., W. R. McGillis, P. Schlosser, D. Perovich, and T. Takahashi (2009), Effects of freezing, growth, and ice cover on gas transport processes in laboratory seawater experiments, *Geophys. Res. Lett.*, *36*, L05603, doi:10.1029/2008GL036318.
Park, J., T. Park, E. J. Yang, D. Kim, M. Y. Gorbunov, H. C. Kim, S. H. Kang, H. C. Shin, S. Lee, and S. Yoo (2013), Early summer iron limitation of phytoplankton photosynthesis in the Scotia Sea as inferred from fast repetition rate fluorometry, *J. Geophys. Res.*, *118*, 3795–3806, doi:10.1002/jgrc.20281.
Reuer, M., B. Barnett, M. Bender, P. Falkowski, and M. Hendricks (2007), New estimates of Southern Ocean biological production rates from O_2/Ar ratios and the triple isotope composition of O2, *Deep Sea Res., Part I*, *54*(6), 951–974.
Rintoul, S. R., and T. W. Trull (2001), Seasonal evolution of the mixed layer in the Subantarctic Zone south of Australia, *J. Geophys. Res.*, *106*(C12), 31,447–31,462.
Sedwick, P. N., and G. R. DiTullio (1997), Regulation of algal blooms in Antarctic shelf waters by the release of iron from melting sea ice, *Geophys. Res. Lett.*, *24*(20), 2515–2518.
Spreen, G., L. Kaleschke, and G. Heygster (2008), Sea ice remote sensing using AMSR-E 89 GHz channels, *J. Geophys. Res.*, *113*, C02S03, doi:10.1029/2005JC003384.
Tortell, P. (2005), Dissolved gas measurements in oceanic waters made by membrane inlet mass spectrometry, *Limnol. Oceanogr.*, *3*, 24–37.
Tortell, P., C. Gueguen, M. C. Long, C. D. Payne, P. A. Lee, and G. R. DiTullio (2011), Spatial variability and temporal dynamics of surface water pCO_2, ΔO_2/Ar and dimethylsulfide in the Ross Sea, Antarctica, *Deep Sea Res., Part I*, *58*, 241–259.
Tortell, P. D., M. C. Long, C. D. Payne, A.-C. Alderkamp, P. Dutrieux, and K. R. Arrigo (2012), Spatial distribution of pCO_2, ΔO_2/Ar and dimethylsulfide (DMS) in polynya waters and the sea ice zone of the Amundsen Sea, Antarctica, *Deep Sea Res., Part II*, *71–76*, 77–93.
Wanninkhof, R. (1992), Relationship between wind speed and gas exchange, *J. Geophys. Res.*, *97*(C5), 7373–7382.